

Ag-based Electrical Contact Material Reinforced by Ti_3AlC_2 Ceramic and Its Derivative $\text{Ti}_3\text{C}_2\text{T}_x$

DING Jianxiang^{1,2,3}, ZHANG Kaige², LIU Dongming^{2,3}, ZHENG Wei¹, ZHANG Peigen¹, SUN Zhengming^{1,2}

(1. Jiangsu Key Laboratory of Advanced Metallic Materials, School of Materials Science and Engineering, Southeast University, Nanjing 211189, China; 2. School of Materials Science and Engineering, Anhui University of Technology, Ma'anshan 243002, China; 3. Key Laboratory of Green Fabrication and Surface Technology of Advanced Metal Materials, Ministry of Education, Anhui University of Technology, Ma'anshan 243002, China)

Abstract: Ag-based electrical contact plays a key role in low-voltage switches, which is intended to substitute the traditional and toxic “universal” contact of Ag/CdO. As a new kind of two-dimensional carbide material with good electrical conductivity and thermal conductivity, $\text{Ti}_3\text{C}_2\text{T}_x$, a representative of MXenes has showed exceptional potential in various fields, including being the reinforcement phase in electrical contact materials to substitute for the toxic CdO. In this work, we successfully prepared Ag/ $\text{Ti}_3\text{C}_2\text{T}_x$ composite by powder metallurgy. Phase and microstructure of the $\text{Ti}_3\text{C}_2\text{T}_x$ and Ti_3AlC_2 were characterized, and their properties, such as electrical resistivity, microhardness, machinability, tensile strength, and anti-arc erosion performance were investigated and compared. The Ag/ $\text{Ti}_3\text{C}_2\text{T}_x$ has a resistivity of $30 \times 10^{-3} \mu\Omega \cdot \text{m}$, 29% lower than that of Ag/ Ti_3AlC_2 ($42 \times 10^{-3} \mu\Omega \cdot \text{m}$) and excellent machinability with intermediate microhardness (64 HV), showing broad application prospect as non-toxic electrical contact materials. Its improved conductivity is mainly attributed to the metallicity of $\text{Ti}_3\text{C}_2\text{T}_x$ itself, the microstructural features, endowed by the deformability of $\text{Ti}_3\text{C}_2\text{T}_x$. However, the tensile strength (32.77 MPa) of Ag/ $\text{Ti}_3\text{C}_2\text{T}_x$ is inferior to that of Ag/ Ti_3AlC_2 (145.52 MPa) due to lack of Al-Ag interdiffusion. The anti-arc erosion performance of Ag/ $\text{Ti}_3\text{C}_2\text{T}_x$ is also unmatched with Ag/ Ti_3AlC_2 due to absence of Al layer. Although the arc erosion resistance of Ag/ $\text{Ti}_3\text{C}_2\text{T}_x$ needs to be further improved uptill now, the significantly improved electrical conductivity makes it a potential substitute of current toxic Ag/CdO material. All results of this work provide an exploration direction for developing new environmentally friendly electrical contact material in the future.

Key words: electrical contact material; MAX phase ceramic; MXene; electrical conductivity; mechanical property; anti-arc erosion performance

As the critical component in low-voltage switching device, Ag-based electrical contacts are widely applied in contactors, breakers and relays, *etc.* The service life of these devices largely depends on the properties of the electrical contact material^[1]. The conventional material “Ag/CdO” has long been preferred because of its outstanding contacting and arc extinction properties since the middle of last century. However, the toxicity of CdO causes serious pollution problems, restricting its applications^[2]. In the past few decades, Cd-free electrical contact materials, such as Ag/SnO₂, Ag/ZnO, Ag/C, Ag/Ni,

have been studied extensively^[3-7]. These substitutes cannot yet emulate Ag/CdO in terms of temperature rise, contact resistivity, machinability, arc erosion resistance, *etc.* Therefore, environment-friendly alternative with properties matching up CdO is in high demand.

Over the past decades, MAX phase^[8-10], combining excellent properties of metal and ceramic, has been widely investigated in various fields^[11-16]. As a representative member of MAX family, Ti_3AlC_2 has been used to reinforce Ag matrix as the electrical contact material^[17-21]. However, the electrical resistivity of the Ag/ Ti_3AlC_2

Received date: 2021-07-02; **Revised date:** 2021-09-28; **Published online:** 2021-11-01

Foundation item: National Natural Science Foundation of China (51731004, 52101064, 52072003); Anhui Provincial Natural Science Foundation (2008085QE195); National Key Research and Development Program of China (2017YFE0301403); Jiangsu Planned Projects for Postdoctoral Research Funds (2020Z158); Natural Science Foundation of Jiangsu Province (BK20201283)

Biography: DING Jianxiang (1987–), male, PhD, lecturer. E-mail: jxding@ahut.edu.cn
丁建翔(1987–), 男, 博士, 讲师. E-mail: jxding@ahut.edu.cn

Corresponding author: ZHANG Peigen, associate professor. E-mail: zhpeigen@seu.edu.cn; SUN Zhengming, professor. E-mail: zmsun@seu.edu.cn
张培根, 副教授. E-mail: zhpeigen@seu.edu.cn; 孙正明, 教授. E-mail: zmsun@seu.edu.cn

composite is not satisfactory, which is initially attributed to the inter-diffusion between Al layer and Ag matrix^[22]. 2011, Gogotsi and Barsoum^[23-24] jointly obtained a new kind of carbide material ($\text{Ti}_3\text{C}_2\text{T}_x$) with two-dimensional structure, coined as MXenes, were produced by selectively etching off Al atom planes from its parent Ti_3AlC_2 . Up to date, $\text{Ti}_3\text{C}_2\text{T}_x$ has received great attentions of many applications^[25-29]. In addition to large specific surface area, $\text{Ti}_3\text{C}_2\text{T}_x$ has good electrical conductivity, thermal-conducting property, and hydrophilicity^[30], and thus it is promising reinforcement for electrical conductive composites. In particular, $\text{Ti}_3\text{C}_2\text{T}_x$ has demonstrated its potential as an additive in composites with polymers (PVA, PAM, PEI, PAN, *etc.*), ceramics (MoS_2 , TiO_2 , *etc.*) and carbon materials (CNT, MWCNT, CNFs, *etc.*)^[31]. Hence, the electric conductive $\text{Ti}_3\text{C}_2\text{T}_x$ is expected to reinforce Ag matrix as a new electrical contact material.

In this study, the application of MXenes to electrical contact material is explored. $\text{Ti}_3\text{C}_2\text{T}_x$ reinforced Ag-based composite was prepared by powder metallurgy, and its overall properties, such as electrical resistivity, hardness, machinability, tensile strength, and anti-arc erosion were investigated and compared with those of Ag-based composite reinforced by Ti_3AlC_2 ceramic. The mechanism of properties difference of these two kinds of samples were also analyzed and concluded. The research results would provide significant data for the design and preparation of the new generation of environment-friendly silver-ceramic composite electrical contact materials in the future.

1 Experimental

Base materials for composites were Ag (99.9%, $\sim 10\ \mu\text{m}$, Xinshengfeng, China) and Ti_3AlC_2 (99.0%, $\sim 10\ \mu\text{m}$, *in-situ* prepared with TiC (99%, $\sim 5\ \mu\text{m}$, Aladdin, China), Ti (99.99%, $\sim 50\ \mu\text{m}$, Aladdin, China), Al (99.7%, $\sim 50\ \mu\text{m}$, Zhongnuo xincai, China). $\text{Ti}_3\text{C}_2\text{T}_x$ was obtained by immersing Ti_3AlC_2 (5 g) into hydrofluoric acid (HF) solution (100 mL, 40% in mass) for 24 h under magnetic

stirring ($40\ ^\circ\text{C}$)^[23]. Ag/10% (in mass) $\text{Ti}_3\text{C}_2\text{T}_x$ ($\text{Ag}/\text{Ti}_3\text{C}_2\text{T}_x$) and Ag/10% (in mass) Ti_3AlC_2 ($\text{Ag}/\text{Ti}_3\text{AlC}_2$) mixtures were individually homogenized by ball milling for 0.5 h with a medium of ethyl alcohol (99.7%, Shanghai Titan Scientific Co. Ltd., China). These two mixtures were subsequently cold-pressed into green bodies (15 mm in diameter, 2 mm in thickness) under 800 MPa, and then heat-treated at $700\ ^\circ\text{C}$ for 2 h in argon atmosphere.

Phase composition of the samples was characterized by X-ray diffraction (XRD, Bruker-AXS D8, Germany). The structure change of Ti_3AlC_2 and $\text{Ti}_3\text{C}_2\text{T}_x$ powders were further characterized by Transmission Electron Microscope (TEM) (FEI, Nova Nano 450, America). Vickers hardness of samples was tested under 0.1 MPa by the micro-hardness tester (FM-700, Future-Tech Corp., Japan). Resistivity of samples was measured by the four probe method (Metra HIT 27 I, Gossen Metrawatt, Germany). Microstructure and chemical compositions were characterized by a scanning electron microscope (SEM, FEI/Philips Sirion 2000, Netherlands), equipped with an energy dispersive spectrometer (EDS, AZtes X-MAX 80). The $\text{Ag}/\text{Ti}_3\text{C}_2\text{T}_x$ and $\text{Ag}/\text{Ti}_3\text{AlC}_2$ bulk materials were processed into the dumbbell-shaped samples with length of 40.0 mm, width of 7.5 mm, middle part width of 4 mm and thickness of 2.0 mm. The tensile strength of both samples was tested at a universal test machine (AGS-X5kN, SHIMADZU, Japan) at a speed of $1\ \text{mm}\cdot\text{min}^{-1}$. Finally, the Ti_3AlC_2 or $\text{Ti}_3\text{C}_2\text{T}_x$ reinforced Ag-based composite electrical contact was installed in commercial contactors and tested under the harsh conditions (400V/100A/AC3, GB14048.4-2010) at Low Voltage Switch Testing Center of Shanghai Electrical Appliance Research Institute.

2 Results and discussion

Fig. 1 shows the phase compositions and microstructures of raw powders (Ti_3AlC_2 and $\text{Ti}_3\text{C}_2\text{T}_x$). Ti_3AlC_2 was

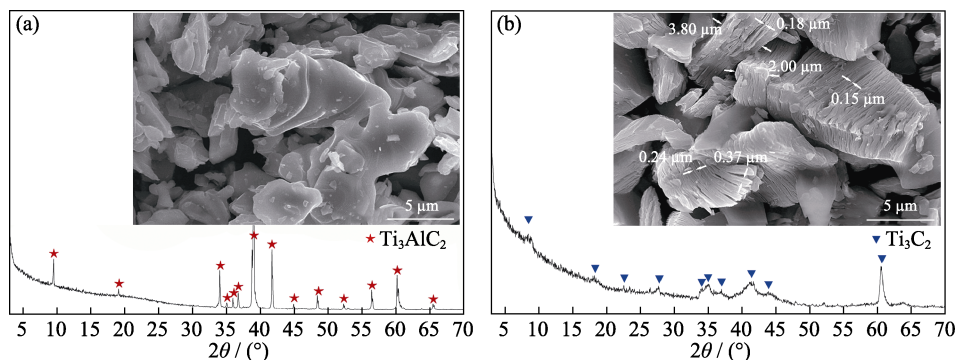


Fig. 1 XRD patterns and morphologies of the raw powders
(a) Ti_3AlC_2 ; (b) $\text{Ti}_3\text{C}_2\text{T}_x$

characterized by granular morphology with smooth surfaces (Fig. 1(a)), and $\text{Ti}_3\text{C}_2\text{T}_x$ exhibited a multilayered morphology with the layer thickness of 0.15–0.37 μm (Fig. 1(b)). Fig. 1(b) obviously shows that the (002) diffraction peak of $\text{Ti}_3\text{C}_2\text{T}_x$ is tilted towards low angle, which also confirms the expansion of $\text{Ti}_3\text{C}_2\text{T}_x$ layer space.

The microstructures and element distributions of Ag/ Ti_3AlC_2 and Ag/ $\text{Ti}_3\text{C}_2\text{T}_x$ composites are displayed in Fig. 2. As shown in Fig. 2(a, c), both reinforcements (Ti_3AlC_2 and $\text{Ti}_3\text{C}_2\text{T}_x$) uniformly distribute in Ag matrices, Ti_3AlC_2 retains the granular morphology while $\text{Ti}_3\text{C}_2\text{T}_x$ takes the stripe-shaped morphology. Fig. 2(b, d) display the element distributions of Ag, Ti and Al in composites, which further confirm that Ti_3AlC_2 and $\text{Ti}_3\text{C}_2\text{T}_x$ take different shapes in Ag matrices. Moreover, slight diffusion of Al with Ag is observed in Ag/ Ti_3AlC_2 (Fig. 2(b)), while a few Al elements detected in Ag/ $\text{Ti}_3\text{C}_2\text{T}_x$ (Fig. 2(d)), which is consistent with the XRD and TEM results.

Ag/ $\text{Ti}_3\text{C}_2\text{T}_x$ composite is further observed at higher magnification SEM image (Fig. 3(a)). It is obvious that the interface between $\text{Ti}_3\text{C}_2\text{T}_x$ and Ag matrices is clear with no trace of cracks and holes, indicating a good physical bonding. However, $\text{Ti}_3\text{C}_2\text{T}_x$ has large contact angle with Ag substrate in the high-temperature wetting experiment (Fig. 3(b)), which confirms the absence of reactive wetting (*i.e.* chemical bonding) between them.

Contact materials are usually manufactured into various shapes, necessitating excellent machinability. A typical negative case is SnO_2 with high hardness leading to the poor machinability of Ag/ SnO_2 , which hinders its substitute for CdO^[32]. Fig. 4 shows the Vickers hardness of Ag/ $\text{Ti}_3\text{C}_2\text{T}_x$, Ag/ Ti_3AlC_2 , and pure Ag (for reference). Ag/ $\text{Ti}_3\text{C}_2\text{T}_x$ possesses intermediate hardness (64 HV), and can be cut into different shapes, including rod, rivet, disc and square (the insert in Fig. 4). The good machinability originates from the 2D structure of $\text{Ti}_3\text{C}_2\text{T}_x$, in which weak van der Waals interaction exists between layers. In addition, contacts usually carry high current density in service, thus a low resistivity is a prerequisite

for potential electrical contact materials. As shown in Fig. 4, the Ag/ $\text{Ti}_3\text{C}_2\text{T}_x$ and Ag/ Ti_3AlC_2 composites own low resistivity ($16 \times 10^{-3} \mu\Omega \cdot \text{m}$ of Ag for reference). In particular, the resistivity of Ag/ $\text{Ti}_3\text{C}_2\text{T}_x$ ($30 \times 10^{-3} \mu\Omega \cdot \text{m}$) is 29% lower than that of Ag/ Ti_3AlC_2 ($42 \times 10^{-3} \mu\Omega \cdot \text{m}$), which is highly meaningful for the practice application.

The improved conductivity of Ag/ $\text{Ti}_3\text{C}_2\text{T}_x$ can be explained from three aspects: higher conductivity of $\text{Ti}_3\text{C}_2\text{T}_x$ than that of Ti_3AlC_2 , enhanced interface bonding between Ag and $\text{Ti}_3\text{C}_2\text{T}_x$, deformability of the stripe-shaped $\text{Ti}_3\text{C}_2\text{T}_x$ in Ag matrices.

Firstly, based on the first-principle band structure calculations, in Ti_3AlC_2 , Ti3d state contributes to the majority of the total densities of states (DOS) at Fermi level; removal of the Al layers from Ti_3AlC_2 results in the redistribution of Ti3d states from broken Ti–Al bonds into delocalized Ti–Ti metallic-like bonding states, leading to the increase of local DOS maximums at Fermi level^[33]. Thus, in MXene ($\text{Ti}_3\text{C}_2\text{T}_x$), the electron density of states near Fermi level ($N(E_f)$) is 1.9–3.2 times higher than that in the corresponding MAX (Ti_3AlC_2)^[34]. Secondly, EDS mapping indicates the existence of O and F elements, which may come from the functional groups (–F, –OH) of $\text{Ti}_3\text{C}_2\text{T}_x$ surface^[35] (Fig. 5).

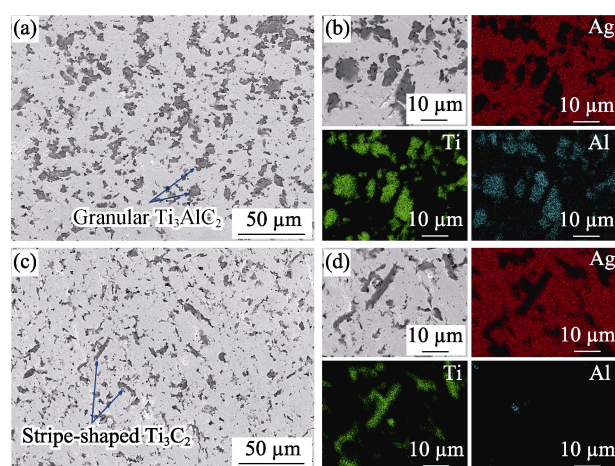


Fig. 2 Microstructures with SEM images (a, c) and element distribution (b, d) of composites (a, b) Ag/ Ti_3AlC_2 ; (c, d) Ag/ $\text{Ti}_3\text{C}_2\text{T}_x$

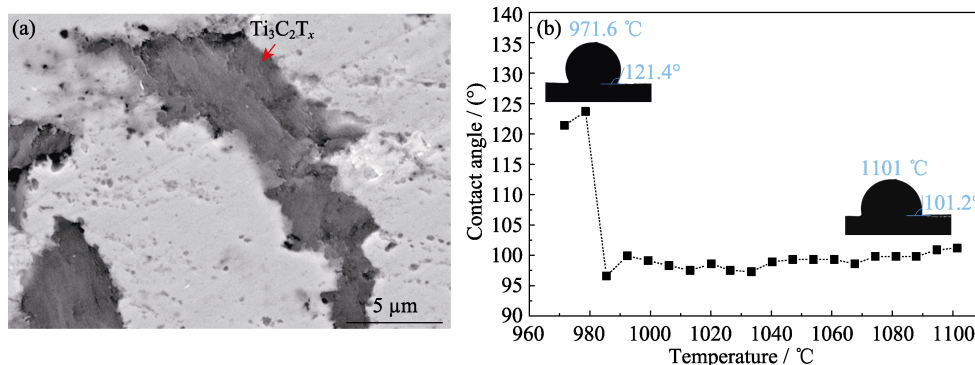


Fig. 3 High-magnification SEM image of $\text{Ti}_3\text{C}_2\text{T}_x$ in Ag matrix (a) and high-temperature wettability of $\text{Ti}_3\text{C}_2\text{T}_x$ with Ag (b) The insets in (b) show optical images of contact angle at different temperatures

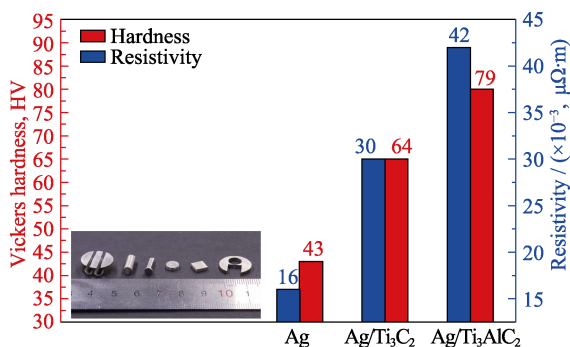


Fig. 4 Machinability, electrical resistivity (blue bar) and Vickers hardness (red bar) of Ag/Ti₃C₂T_x and Ag/Ti₃AlC₂, compared with those of Ag. The insert is pieces cut from Ag/Ti₃C₂T_x; colorful figure is available on website

Generally, the hydrophilicity of -F/-OH functional groups is beneficial to the bonding between Ti₃C₂T_x and metal matrices^[34], which avoids the similar phenomenon of poor interface bonding between carbon nanotubes, fibers and metal matrices^[36]. In addition, the SEM observation also displays the tight bonding between Ti₃C₂T_x and Ag matrices without obvious cracks and holes, as shown in Fig. 2(c) and Fig. 3(a). Hence, the uniform microstructure and good bonding of Ag/Ti₃C₂T_x improved the conductivity. Thirdly, as shown in Fig. 2(b, d), the microstructure of stripe-shaped Ti₃C₂T_x is obviously different from that of granular Ti₃AlC₂ in Ag matrices. The 2D layered structure of Ti₃C₂T_x facilitates its deformability during preparation. The Ti₃C₂T_x was cold compacted into the stripe-like Ti₃C₂T_x (average thickness of ~ 3 μm), whereas Ti₃AlC₂ retains its original shape (average diameter of ~ 10 μm). In contrast with granular Ti₃AlC₂, the stripe-shaped Ti₃C₂T_x has smaller cross-sectional area perpendicular to the current direction, minimizing the scattering section for electrons and the resistance to the electron transmission. In summary, the excellent machinability and electrical conductivity makes

Ag/Ti₃C₂T_x a promising substitute for Ag/CdO.

However, as shown in Fig. 6, the maximum tensile strength of Ag/Ti₃C₂T_x composite (32.77 MPa) is far less than that of Ag/Ti₃AlC₂ composite (145.52 MPa). The superior tensile strength of Ag/Ti₃AlC₂ composite derives from the interdiffusion between the active Al atomic layer with Ag matrices. On the contrary, the absence of Al layer leads to the weaker interface bonding strength between Ti₃C₂T_x and Ag matrices, which finally deteriorates the mechanical property of the entire Ag/Ti₃C₂T_x composite.

In order to further investigate the property of Ag/Ti₃C₂T_x, electrical arc discharging experiments were carried out on this contact surface under a harsh condition (AC-3, 100 A, 400 V, GB14048.4-2010). The Ag/Ti₃C₂T_x contact failed to make and break after 1233 times arc discharging. The optical image shows that the shape of contact remains well with some dents and protuberances (Fig. 7(a, b)). The surface morphologies of Ag/Ti₃C₂T_x contact after arc erosion are subsequently exhibited in Fig. 7(c), complete edge and flat surface were further confirmed by SEM. Some Ag spheres, solidified Ag blocks, and small cracks were observed at high-magnification SEM image (Fig. 7(d)). Fig. 7(e-h) exhibit the microstructure and chemical composition of Ag/Ti₃C₂T_x contact surface. There are many irregular dark blocks surrounded by little bright particles (Fig. 7(e)). As shown in Fig. 7(f), area 1 (white block) contains large amount of Ti, O, F with trace of Ag and Al, which may be attributed to the Ti-O-F mixture produced by electrical arc erosion to Ti₃C₂T_x. Area 2 (bright particles) is mainly composed of Ag, F, and O. It is deduced that the Ag-O-F mixture was produced by the absorption of O₂ in liquid Ag and reaction with -F function group of Ti₃C₂T_x. Fig. 7(h) displays two types of spheroid particles at magnified SEM image. EDS analysis results showed that both the particles contained vast N element, showing that these two particles were composed of Ag-O-F-N.

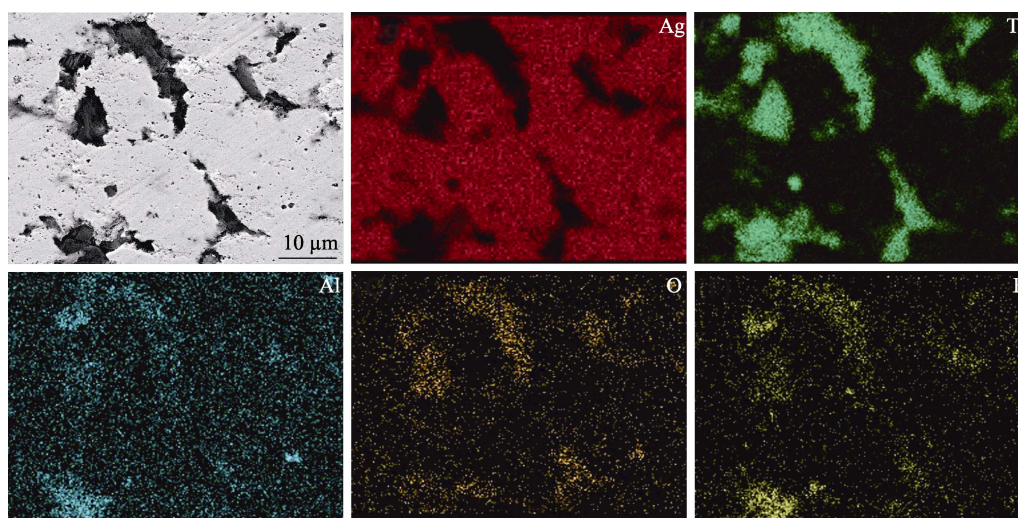


Fig. 5 Morphology and element distributions of Ag/Ti₃C₂T_x composite in high-magnification SEM image

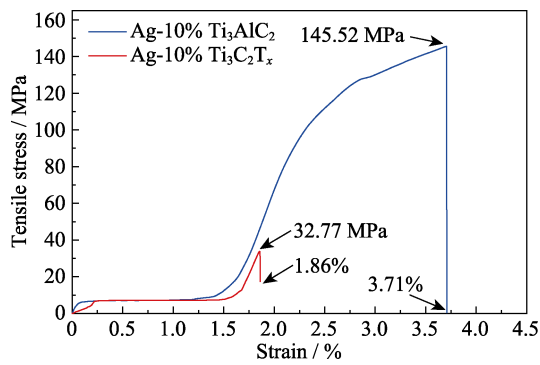


Fig. 6 Tensile properties of Ag-based composites reinforced by different reinforced phase materials

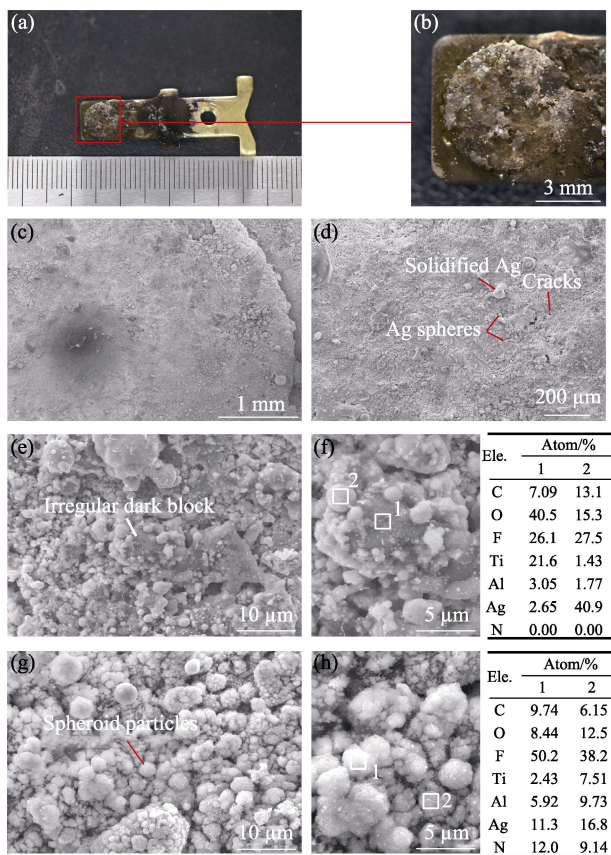


Fig. 7 Surface morphology, microstructure and chemical composition of $Ag/Ti_3C_2T_x$ contact after arc erosion (a, b) Optical image and magnified image; (c, d) Surface morphology; (e-h) Microstructures and chemical composition

The relative mass loss of $Ag/Ti_3C_2T_x$ (54% after 1233 times arc discharging) is considerably more than that of Ag/Ti_3AlC_2 (0.82% after 3000 times arc discharging), which is also attributed to the absence of Al layer in Ti_3AlC_2 . As analyzed previously, the lack of Al-Ag interdiffusion leads to the weak bonding strength of $Ti_3C_2T_x$ with Ag, and thus decrease the mechanical property of composite, which accordingly impairs the resistance to electrical arc impact damage. In addition, the absence of Al-Ag interdiffusion also results in the poor wettability of $Ti_3C_2T_x$ with Ag during the electrical arc discharging

and consequently decreased viscosity of molten pool, finally deteriorating the resistance to the material transfer of $Ti_3C_2T_x$ and Ag under electrical arc high-temperature. Nonetheless, there is still space for further improvement of the arc erosion resistance of $Ag/Ti_3C_2T_x$ with superior electrical conductivity by the composition design, structure optimization, technique promotion in the following work.

3 Conclusions

In this work, Ag-based electrical contact materials, reinforced by Ti_3AlC_2 ceramic and its derivative ($Ti_3C_2T_x$), were successfully prepared by powder metallurgy. The microstructure, chemical composition, hardness, conductivity, machinability, mechanical property and erosion resistance of Ag/Ti_3AlC_2 and $Ag/Ti_3C_2T_x$ composites were investigated and compared. The main conclusions are as follows:

- 1) Stripe-like $Ti_3C_2T_x$ uniformly distributes in $Ag/Ti_3C_2T_x$ composite.
- 2) In contrast with Ag/Ti_3AlC_2 , $Ag/Ti_3C_2T_x$ has lower resistivity ($30 \times 10^{-3} \mu\Omega \cdot m$), 29% lower than that of Ag/Ti_3AlC_2 . The superior conductivity of $Ag/Ti_3C_2T_x$ results from the stronger metallicity of $Ti_3C_2T_x$, uniform microstructure, and smaller cross-sectional area of $Ti_3C_2T_x$ in the composite.
- 3) The moderate hardness and excellent machinability of $Ag/Ti_3C_2T_x$ are also satisfactory for electrical contact materials.
- 4) The tensile strength (32.77 MPa) of $Ag/Ti_3C_2T_x$ composite is inferior to that of Ag/Ti_3AlC_2 (145.52 MPa) due to the lack of Al-Ag interdiffusion.
- 5) $Ag/Ti_3C_2T_x$ shows moderate arc erosion resistance with production of Ti-O-F, Ag-O-F, and Ag-O-F-N mixture, which is inferior to that of Ag/Ti_3AlC_2 , and needs to be further improved.

References:

- [1] FEHIM F, HUSEYIN U. Microstructure, hardness and electrical properties of silver-based refractory contact materials. *Materials & Design*, 2003, **24**(7): 489–492.
- [2] HAUNER F, JEANNOT D, MCNEILLY K, *et al.* Advanced $AgSnO_2$ Contact Materials for the Replacement of $AgCdO$ in High Current Contactors. Proceedings of the Forty-Sixth IEEE Holm Conference on Electrical Contacts, New York: IEEE, 2000: 225–230.
- [3] NILSSON O, HAUNER F, JEANNOT D. Replacement of $AgCdO$ by $AgSnO_2$ in DC contactors. Proceedings of the 50th IEEE Holm Conference on Electrical Contacts/the 22nd International Conference on Electrical Contacts, New York: IEEE, 2004: 70–74.
- [4] GAVRILIU S, LUNGU M, ENESCU E, *et al.* A comparative study concerning the obtaining and using of some Ag-CdO, Ag-ZnO and Ag-SnO₂ sintered electrical contact materials. *Optoelectronics and Advanced Materials-Rapid Communications*, 2009, **3**(7): 688–692.
- [5] REHANI B, JOSHI P B, KHANNA P K. Fabrication of silver-

- graphite contact materials using silver nanopowders. *Journal of Materials Engineering and Performance*, 2010, **19**(1): 64–69.
- [6] SWINGLER J. Performance and arcing characteristics of Ag/Ni contact materials under DC resistive load conditions. *IET Science, Measurement & Technology*, 2011, **5**(2): 37–45.
- [7] ZHANG H, WANG X H, LI Y P, *et al.* Preparation and characterization of silver-doped graphene-reinforced silver matrix bulk composite as a novel electrical contact material. *Applied Physics A*, 2019, **125**(2): 86.
- [8] SUN Z M. Progress in research and development on MAX phases: a family of layered ternary compounds. *International Materials Reviews*, 2011, **56**(3): 143–166.
- [9] ZHENG G M, HUANG Z Y, YU Q, *et al.* Microstructural and mechanical properties of $Ti_{1-x}Ni_x(Al, Ti)/Ni$ functionally graded composites fabricated from Ti_3AlC_2 and Ni powders. *Metals and Materials International*, 2020, **26**(6): 905–913.
- [10] WANG X H, ZHOU Y C. Layered machinable and electrically conductive Ti_2AlC and Ti_3AlC_2 ceramics: a review. *Journal of Materials Science & Technology*, 2010, **26**(5): 385–416.
- [11] DING J X, TIAN W B, ZHANG P G, *et al.* Arc erosion behavior of Ag/ Ti_3AlC_2 electrical contact materials. *Journal of Alloys and Compounds*, 2018, **740**: 669–676.
- [12] DING J X, TIAN W B, ZHANG P G, *et al.* Preparation and arc erosion properties of Ag/ Ti_2SnC composites under electric arc discharging. *Journal of Advanced Ceramics*, 2019, **8**(1): 90–101.
- [13] DING J X, HUANG P Y, ZHA Y H, *et al.* High-purity Ti_2AlC powder: preparation and application in Ag-based electrical contact materials. *Journal of Inorganic Materials*, 2020, **35**(6): 729–734.
- [14] DING J X, TIAN W B, WANG D D, *et al.* Arc erosion and degradation mechanism of Ag/ Ti_2AlC composite. *Acta Metallurgica Sinica*, 2019, **55**(5): 627–637.
- [15] DING J X, TIAN W B, WANG D D, *et al.* Microstructure evolution, oxidation behavior and corrosion mechanism of Ag/ Ti_2SnC composite during dynamic electric arc discharging. *Journal of Alloys and Compounds*, 2019, **785**: 1086–1096.
- [16] GONG Y M, TIAN W B, ZHANG P G, *et al.* Slip casting and pressureless sintering of Ti_3AlC_2 . *Journal of Advanced Ceramics*, 2019, **8**: 367–376.
- [17] HUANG X C, FENG Y, QIAN G, *et al.* Erosion behavior of Ti_3AlC_2 cathode under atmosphere air arc. *Journal of Alloys and Compounds*, 2017, **727**: 419–427.
- [18] HUANG X C, FENG Y, QIAN G, *et al.* Influence of breakdown voltages on arc erosion of a Ti_3AlC_2 cathode in an air atmosphere. *Ceramics International*, 2017, **43**(13): 10601–10605.
- [19] HUANG X C, FENG Y, QIAN G, *et al.* Arc corrosion behavior of Cu- Ti_3AlC_2 composites in air atmosphere. *Science China Technological Sciences*, 2018, **61**(4): 551–557.
- [20] LIU M M, CHEN J L, CUI H, *et al.* Ag/ Ti_3AlC_2 composites with high hardness, high strength and high conductivity. *Materials Letters*, 2018, **213**: 269–273.
- [21] LIU M M, CHEN J L, CUI H, *et al.* Temperature-driven deintercalation and structure evolution of Ag/ Ti_3AlC_2 composites. *Ceramics International*, 2018, **44**(15): 18129–18134.
- [22] DING J X, TIAN W B, WANG D D, *et al.* Corrosion and degradation mechanism of Ag/ Ti_3AlC_2 composites under dynamic electric arc discharging. *Corrosion Science*, 2019, **156**: 147–160.
- [23] NAGUIB M, KURTOGLU M, PRESSER V, *et al.* Two-dimensional nanocrystals produced by exfoliation of Ti_3AlC_2 . *Advanced Materials*, 2011, **23**(37): 4248–4253.
- [24] ANASORI B, LUKATSKAYA M R, GOGOTSI Y. 2D metal carbides and nitrides(MXenes) for energy storage. *Nature Reviews Materials*, 2017, **2**(2): 16098.
- [25] NAGUIB M, COME J, DYATKIN B, *et al.* MXene: a promising transition metal carbide anode for lithium-ion batteries. *Electrochemistry Communications*, 2012, **16**(1): 61–64.
- [26] ZHENG W, ZHANG P G, CHEN J, *et al.* In situ synthesis of CNTs/ Ti_3C_2 hybrid structures by microwave irradiation for high-performance anodes in lithium ion batteries. *Journal of Materials Chemistry A*, 2018, **6**(8): 3543–3551.
- [27] SHAHZAD F, ALHABEB M, HATTER C B, *et al.* Electromagnetic interference shielding with 2D transition metal carbides(MXenes). *Science*, 2016, **353**(6304): 1137–1140.
- [28] YU X F, LI Y C, CHENG J B, *et al.* Monolayer Ti_2CO_2 : a promising candidate for NH_3 sensor or capturer with high sensitivity and selectivity. *ACS Applied Materials & Interfaces*, 2015, **7**(24): 13707–13713.
- [29] ZHANG H, WANG L, CHEN Q, *et al.* Preparation, mechanical and anti-friction performance of MXene/polymer composites. *Materials & Design*, 2016, **92**: 682–689.
- [30] LEI J C, ZHANG X, ZHOU Z. Recent advances in MXene: preparation, properties, and applications. *Frontiers of Physics*, 2015, **10**(3): 276–286.
- [31] NG V M H, HUANG H, ZHOU K, *et al.* Recent progress in layered transition metal carbides and or nitrides (MXenes) and their composites-synthesis and applications. *Journal of Materials Chemistry A*, 2017, **5**(7): 3039–3068.
- [32] WANG Y P, LI H Y. Improved workability of the nanocomposited Ag SnO_2 contact material and its microstructure control during the arcing process. *Metallurgical and Materials Transactions A*, 2017, **48**(2): 609–616.
- [33] SHEIN I R, IVANOVSKII A L. Graphene-like titanium carbides and nitrides $Ti_{n+1}C_n$, $Ti_{n+1}N_n$ ($n=1, 2$, and 3) from de-intercalated MAX phases: first-principles probing of their structural, electronic properties and relative stability. *Computational Materials Science*, 2012, **65**: 104–114.
- [34] NAGUIB M, MOCHALIN V N, BARSOUM M W, *et al.* 25th anniversary article: MXenes: a new family of two-dimensional materials. *Advanced Materials*, 2014, **26**(7): 992–1005.
- [35] NAGUIB M, MASHTALIR O, CARLE J, *et al.* Two-dimensional transition metal carbides. *ACS Nano*, 2012, **6**(2): 1322–1331.
- [36] ZHANG X, LI S F, PAN B, *et al.* Regulation of interface between carbon nanotubes-aluminum and its strengthening effect in CNTs reinforced aluminum matrix nanocomposites. *Carbon*, 2019, **155**: 686–696.

Ti_3AlC_2 陶瓷及其衍生物 $Ti_3C_2T_x$ 增强的 Ag 基电接触材料

丁健翔^{1,2,3}, 张凯歌², 柳东明^{2,3}, 郑伟¹, 张培根¹, 孙正明^{1,2}

(1. 东南大学 材料科学与工程学院, 先进金属材料重点实验室, 南京 211189; 2. 安徽工业大学 材料科学与工程学院, 马鞍山 243002; 3. 先进金属材料绿色制备与表面技术教育部重点实验室(安徽工业大学), 马鞍山 243002)

摘 要: 银基电触头在低压开关领域扮演重要角色。作为一种具有良好导电导热性能的新型二维碳化物材料, MXene 家族典型代表材料($Ti_3C_2T_x$)在多个领域显示出极大的应用潜力。 $Ti_3C_2T_x$ 有望作为一种新型环保银基电触头增强相材料。本研究采用粉末冶金法制备了 Ag/ $Ti_3C_2T_x$ 复合材料, 并对 $Ti_3C_2T_x$ 和 Ti_3AlC_2 的物相和微观结构进行表征。同时研究了 $Ti_3C_2T_x$ 增强 Ag 基复合材料的综合性能, 包括电阻率、显微硬度、机械加工性能、抗拉强度和抗电弧侵蚀性能, 并与 Ti_3AlC_2 增强 Ag 基复合材料进行了比较。Ag/ $Ti_3C_2T_x$ 的电阻率($30 \times 10^{-3} \mu\Omega \cdot m$)相对于 Ag/ Ti_3AlC_2 ($42 \times 10^{-3} \mu\Omega \cdot m$)降低了 29%。Ag/ $Ti_3C_2T_x$ 硬度适中(64 HV), 具有良好的可加工性, 作为无毒电触头材料应用前景广阔。Ag/ $Ti_3C_2T_x$ 复合材料导电性能的提高主要归因于 $Ti_3C_2T_x$ 本身优异的金属性以及由 $Ti_3C_2T_x$ 微观结构特征带来的可变形性。由于缺乏 Al-Ag 相互扩散, Ag/ $Ti_3C_2T_x$ 复合材料的拉伸强度(32.77 MPa)明显低于 Ag/ Ti_3AlC_2 复合材料(145.52 MPa)。正因为缺失 Al 层, Ag/ $Ti_3C_2T_x$ 的抗电弧侵蚀性能也无法与 Ag/ Ti_3AlC_2 相媲美。尽管 Ag/ $Ti_3C_2T_x$ 的抗电弧侵蚀性能有待进一步提高, 但优异的导电性使其有望替代有毒的 Ag/CdO 电接触材料。该研究结果为开发新型环保电触头材料提供了新的探索方向。

关 键 词: 电接触材料; MAX 相陶瓷; MXene; 导电性; 力学性能; 抗电弧侵蚀性能

中图分类号: TG148 **文献标志码:** A